RESEARCH ARTICLE SUMMARY

TRANSCRIPTION

Term-seq reveals abundant ribo-regulation of antibiotics resistance in bacteria

Daniel Dar, Maya Shamir, J. R. Mellin, Mikael Koutero, Noam Stern-Ginossar, Pascale Cossart, Rotem Sorek*

INTRODUCTION: Riboswitches and attenuators are cis-regulatory RNA elements (ribo-regulators), which in most cases control bacterial gene expression via ligand-mediated, premature transcription termination. Depending on the presence or absence of the specific ligand, the formation of a transcription terminator upstream of the gene causes transcription to abort prematurely, generating short unproductive transcripts. In response to changes in the metabolite concentrations, the structure of the ribo-regulator is altered, destabilizing the terminator and allowing read-through into the gene, thus resulting in expression of the full-length mRNA. These ribo-regulators play central roles in bacterial physiology and virulence and have been used for synthetic biology applications as well as recognized as therapeutic targets for antibiotics.

RATIONALE: Despite the importance of riboswitches and attenuators, there is currently no experimental high-throughput method for the discovery of such ribo-regulators across bacterial genomes. Furthermore, given a metabolite or ligand of interest, until now there was no efficient experimental approach to identify natural riboswitches or attenuators that sense and respond to it.

RESULTS: We developed term-seq, a method that enables quantitative mapping of all exposed RNA 3′ ends in bacteria and allows unbiased, genome-wide identification of genes that are regulated by premature transcription termination. This method quantitatively measures the in vivo activities of all expressed ribo-regulators in a given genome simultaneously and under physiological conditions, thus enabling high-throughput discovery of ribo-regulators that respond to a metabolite of interest. Application of term-seq to the model bacteria *Bacillus subtilis*, *Listeria monocytogenes*, and *Enterococcus faecalis* detected the vast majority of known riboswitches as well as multiple previously unidentified regulators that function via conditional termination.

ON OUR WEBSITE

Read the full article at http://dx.doi.org/10.1126/science.aad9822

We demonstrate the utility of our approach by screening for ribo-regulators that specifically respond to small antibiotic molecules. We found that numerous antibiotics resistance genes, in both pathogenic bacteria and in the human microbiome, are regulated via termination-based ribo-regulators that allow read-through when the antibiotic is present in the cell.

Focusing on *lmo0919*, one of the antibiotic-regulated genes we detected in *Listeria monocytogenes*, revealed that this locus confers specific resistance to the translation-inhibiting antibiotic lincomycin. In the absence of the antibiotic, transcription is terminated prematurely by the ribo-regulator. However, upon exposure to lincomycin, drug-inhibited ribosomes stall over a conserved three-amino-acid upstream open reading frame found within the ribo-regulator, thus triggering a conformational change in the transcriptional terminator and inducing the expression of the full-length mRNA that encodes the resistance gene.

CONCLUSION: These results describe a high-throughput method for ribo-regulator discovery in either bacterial monocultures or complex bacterial communities such as the human microbiome. Furthermore, they reveal a broad role for conditional termination in regulating multiple classes of antibiotic resistance genes in the human microbiome and provide a general tool for discovering riboswitches and attenuators that respond to specific metabolites of choice. ■

A Genome-wide discovery of riboswitches and attenuators (ribo-regulators) via high precision mapping of RNA 3' ends (term-seq)

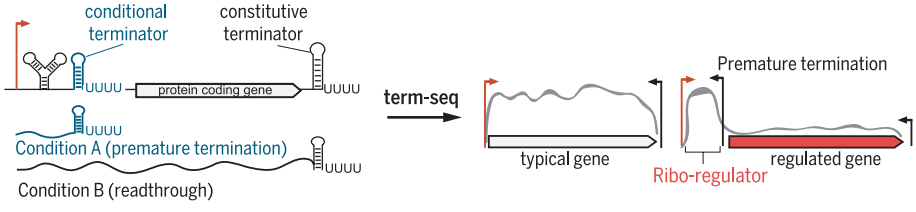

Discovery of antibiotic-responsive ribo-regulators in pathogenic and commensal bacteria

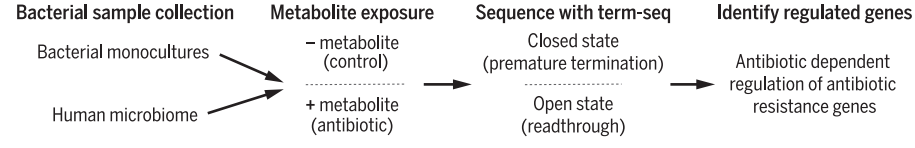

B Mechanism of the *L. monocytogenes lmo0919* ribo-regulator

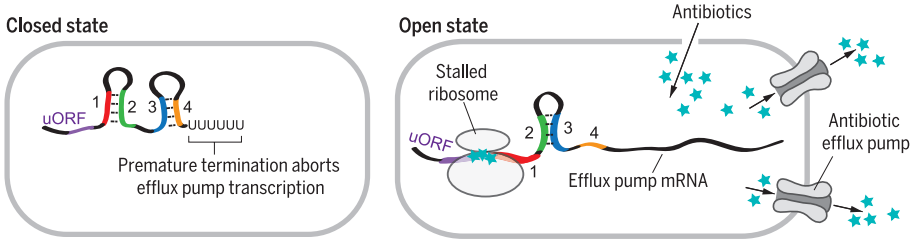

Genome-wide discovery of antibiotic-responsive ribo-regulation in bacteria. (**A**) Direct mapping of RNA 3′ ends reveals gene regulation by conditional termination in a genome-wide manner. Differential sequencing of monoculture or complex bacterial communities under metabolite-rich and -poor conditions (metabolite in this case being an antibiotic) detects ribo-regulators that specifically respond to the metabolite. (**B**) Mechanism of regulation of the *Listeria monocytogenes lmo0919* antibiotic responsive ribo-regulator.

The list of author affiliations is available in the full article online.
*Corresponding author. E-mail: rotem.sorek@weizmann.ac.il
Cite this article as D. Dar *et al.*, *Science* 352, aad9822 (2016). DOI: 10.1126/science.aad9822

RESEARCH ARTICLE

TRANSCRIPTION

Term-seq reveals abundant ribo-regulation of antibiotics resistance in bacteria

Daniel Dar,[1] Maya Shamir,[1] J. R. Mellin,[2,3,4] Mikael Koutero,[2,3,4] Noam Stern-Ginossar,[1] Pascale Cossart,[2,3,4] Rotem Sorek[1]*

Riboswitches and attenuators are cis-regulatory RNA elements, most of which control bacterial gene expression via metabolite-mediated, premature transcription termination. We developed an unbiased experimental approach for genome-wide discovery of such ribo-regulators in bacteria. We also devised an experimental platform that quantitatively measures the in vivo activity of all such regulators in parallel and enables rapid screening for ribo-regulators that respond to metabolites of choice. Using this approach, we detected numerous antibiotic-responsive ribo-regulators that control antibiotic resistance genes in pathogens and in the human microbiome. Studying one such regulator in *Listeria monocytogenes* revealed an attenuation mechanism mediated by antibiotic-stalled ribosomes. Our results expose broad roles for conditional termination in regulating antibiotic resistance and provide a tool for discovering riboswitches and attenuators that respond to previously unknown ligands.

Riboswitches and attenuators are 5′ untranslated region (5′UTR)–residing, cis-regulatory RNA elements (ribo-regulators) that tune gene expression in bacteria by sensing key metabolites, amino acids, nucleotides, and ions (*1*–*6*). These RNA elements can regulate the expression of the downstream gene either at the transcription or the translation level. When riboswitches and attenuators control transcription, they usually generate a condition-specific, regulated transcriptional terminator so that termination results in a prematurely aborted transcript, whereas read-through generates a full-length, productive mRNA (Fig. 1A) (*5*). In the case of riboswitches, the 5′UTR RNA sensor differentially folds to form a terminator or an antiterminator in the presence or absence of a regulating metabolite, respectively; in attenuators, the formation of a transcriptional terminator is mediated by the rate of translation of an upstream open reading frame (uORF), as exemplified in the Trp operon (*4*). Regulation by conditional termination controls key processes in bacteria, including core metabolism (*7*, *8*), motility (*9*), biofilm formation (*9*, *10*), and virulence (*11*, *12*). Riboswitches enable optimization of metabolite production in bacterial expression systems (*13*, *14*), are readily applicable components for synthetic biology applications (*15*, *16*), and also form potential therapeutic targets for new antibiotics (*17*, *18*).

Only ~25 classes of naturally occurring riboswitches have been described to date, although it is estimated that hundreds more exist in bacteria (*19*). Almost all known riboswitches have been discovered via comparative genomics–based approaches comparing intergenic regions across bacterial phyla (*20*). Once a conserved 5′UTR is detected, its possible ligand is predicted on the basis of the identity of the downstream gene, and these predictions are then subject to extensive in vitro verification. This approach has identified riboswitches conserved across a wide phylogenetic range (*19*). However, most of the yet-to-be-discovered elements are predicted to be restricted to specific clades of bacteria, and for such elements, current conservation-based approaches are not appropriate (*19*). We currently lack an experimental method that enables genome-wide discovery of riboswitches and conditional termination regulators. Furthermore, given a metabolite of interest, there is no efficient approach that can identify natural riboswitches or attenuators that sense and respond to it.

Genome-wide mapping of RNA 3′ termini via term-seq

We developed an unbiased experimental approach for genome-wide discovery of conditional, regulated transcriptional termination in bacteria. For this, we first mapped all RNA termini that are present in the cell at a given condition. As opposed to eukaryotic RNA, in which the presence of the nearly universal polyadenylate tail allows direct reverse transcription priming from the 3′ end, the absence of 3′ polyadenylation in bacterial mRNAs makes 3′ ends–mapping challenging (*21*, *22*). We developed a RNA-sequencing (RNA-seq) protocol (denoted here "term-seq") that directly sequences exposed RNA 3′ ends in bacteria, yielding a genome-wide map of RNA termini (Fig. 1B) (*23*). Applying term-seq to a large set of synthetic transcripts mixed in various, predetermined concentrations verified that term-seq accurately reconstitutes the exact 3′ end termini in a highly quantitative manner (fig. S1).

We applied term-seq on *Bacillus subtilis* grown in rich media. The sequencing reads resulting from the term-seq protocol showed >50-fold enrichment for mapping to intergenic regions, implying that sites mapped via term-seq represent native RNA termini existing in the cell (Fig. 1, C and D) (*23*). Associating each gene with its respective term-seq–inferred termination position in the downstream intergenic region led to identification of 1443 transcript termini (Fig. 1E and table S1), the vast majority of which conformed to the sequence and structural features of rho-independent transcriptional terminators (Fig. 1, F and G, and fig. S2) (*23*). These results demonstrate the ability of term-seq to map RNA termini to the single-base resolution across the bacterial genome.

A platform for the discovery of genes regulated by conditional termination

We next sought to examine whether term-seq can be used to identify regulated, premature termination events. Genes that are transcriptionally regulated by riboswitches and attenuators will present a premature termination site within their 5′UTR, downstream to the transcription start site (TSS). We therefore also mapped TSSs across the *B. subtilis* genome using a genome-wide 5′ end sequencing protocol (*23*–*25*) and included standard RNA-seq coverage data so as to gain a comprehensive view of the *B. subtilis* transcriptome (Fig. 1E) (*23*). Examining known *B. subtilis* riboswitches showed reproducible premature termination sites at the 5′ UTR, supporting that such sites can be indicative of riboswitch activity (Fig. 2, A and B).

To assess the sensitivity of this method in revealing genes controlled by regulated termination, we searched for all genes that contained a reproducible term-seq site within their 5′UTRs (*23*). This search recovered 49 (92%) of the 53 transcriptional units (TUs) regulated by known riboswitches in the *B. subtilis* genome (Fig. 2C and table S2) (*23*). Four known riboswitch-regulated genes escaped detection, either because they were under the control of multiple consecutive riboswitches, lacked a mapped TSS, or because of an annotation error that placed the riboswitch within a misannotated ORF (fig. S3). These results therefore show a high sensitivity for our method in mapping riboswitches in a genome-wide manner.

Overall, our search retrieved 82 candidate regulatory elements, of which 64 (78%) were mapped to previously reported elements (Fig. 2C and table S2). In addition to the 49 known riboswitches, we also recovered 11 cases of conditional termination known to be regulated by RNA-binding antitermination proteins, including TRAP (*26*), GlpP (*27*), PyrR (*28*), and PTS system proteins (*29*). We also identified one case of known attenuation

[1]Department of Molecular Genetics, Weizmann Institute of Science, Rehovot 76100, Israel. [2]Institut Pasteur, Unité des Interactions Bactéries-Cellules, Paris, F-75015 France. [3]INSERM, U604, Paris, F-75015 France. [4]Institut National de la Recherche Agronomique, USC2020, Paris, F-75015 France.
*Corresponding author. E-mail: rotem.sorek@weizmann.ac.il

(*30*), as well as three elements (the *rimP*, *Pan*, and *vmlR* leaders) predicted as cis-regulatory elements in *B. subtilis* but for which the mechanism of regulation is unknown (*20*, *31*, *32*).

Because *B. subtilis* is a highly studied model organism, it has one of the best annotated genomes in the bacterial domain. Nevertheless, we detected 18 previously unidentified elements predicted to regulate gene expression by premature termination (Fig. 2C and tables S2 and S3). These included predicted regulatory elements upstream of the formate dehydrogenase gene *yrhE* (Fig. 2D); the guanosine 5′-monophosphate (GMP) synthase gene *guaA*;*yfnI*, a gene responsible for the biosynthesis of the polyglycerolphosphate moiety of lipoteichoic acid; and *yxjB*, a 23*S* ribosomal RNA (rRNA) (guanine748-N1)-methyltransferase predicted to confer resistance to macrolide antibiotics (Fig. 2E). The various functions encoded by the genes newly associated with these regulators, and the lack of homology to any known riboswitch or other RNA elements in the RNA family database (Rfam) (*33*), suggest that these regulatory elements may respond to previously unidentified ligands, antitermination proteins, or attenuation principles.

We then applied term-seq on *Listeria monocytogenes*, a foodborne pathogen that causes gastroenteritis and can lead to severe sepsis and meningitis in immunocompromised and elderly patients and abortions in pregnant women (*34*), and *Enterococcus faecalis*, a causal agent of community and nosocomial infections, including endocarditis and bacteremia (*35*). Similar to *B. subtilis*, in both pathogens term-seq detected most of the known riboswitches that function via regulated termination, as well as predicted, previously unidentified regulators (Fig. 2, C and F to I, and tables S4 and S5). In *L. monocytogenes*, many of the elements we detected were previously annotated as small RNAs or as potential cis-acting regulatory 5′UTRs (*25*, *36*); our data supports that they are indeed cis-acting regulators (Fig. 2, F and G, and table S4). The conditional termination–based elements we

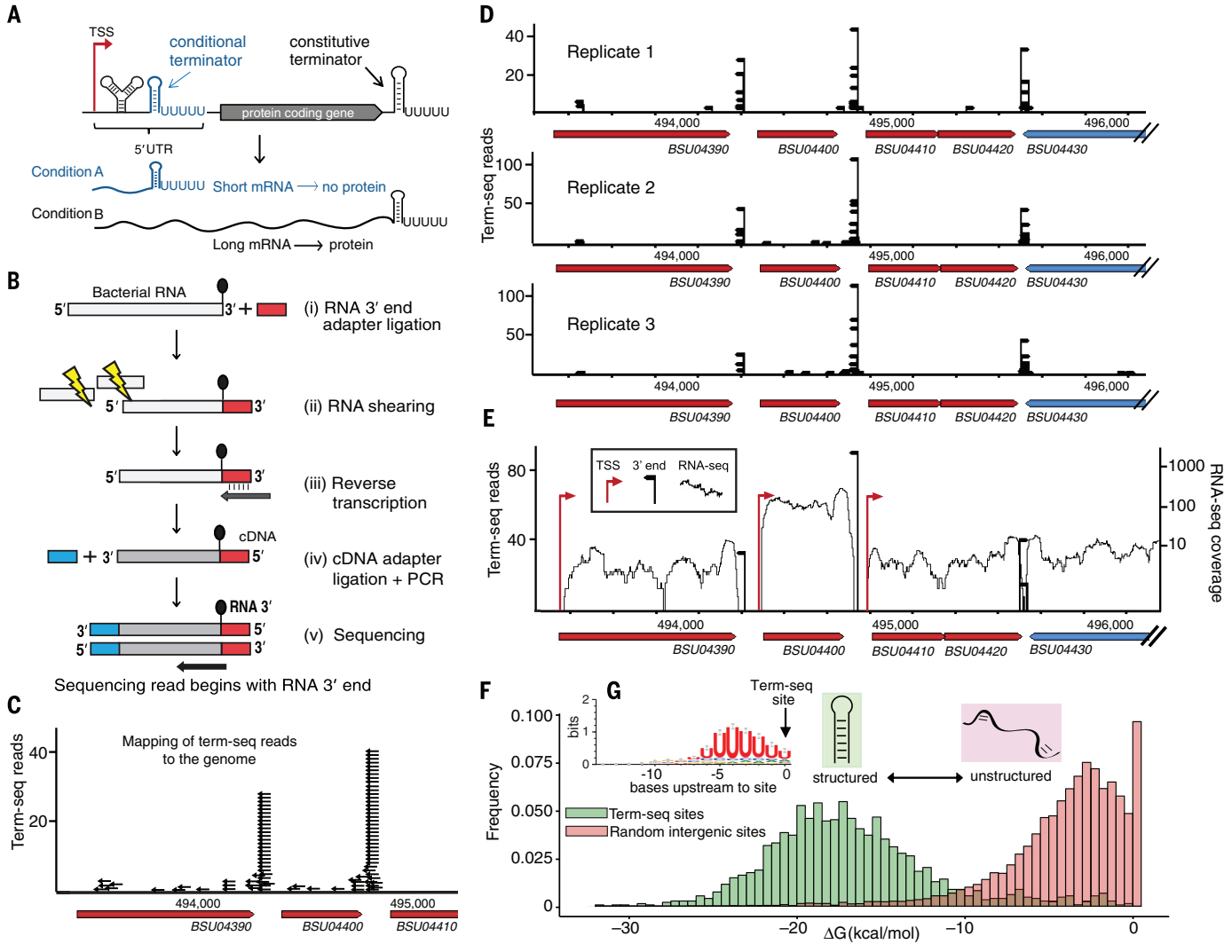

Fig. 1. Term-seq maps RNA termini across the genome. (**A**) Regulation by conditional termination in bacteria. A model 5′ UTR containing a ribo-regulator (riboswitch, protein-binding leader, or attenuator) that differentially folds to generate a condition-specific premature terminator. (**B**) Schematic representation of the term-seq protocol. (**C**) Mapping of term-seq reads to the genome yields a typical pattern in which the majority of reads map to discrete intergenic positions marking RNA 3′ ends. Black arrows represent individual mapped reads. (**D**) Data from three biological replicates over a representative 3-kb window of the *B. subtilis* genome show reproducibility. Black arrowheads represent positions supported by term-seq reads, with arrow height (*y* axis) representing the number of reads supporting the position. (**E**) Multilayered RNA sequencing data provides an integrative view of the bacterial transcriptome. Black arrowheads represent predicted term-seq termination sites, with arrow height indicating the average number of reads in three biological replicates. Black curve represents RNA-seq coverage. Red arrowheads mark the position of TSSs, as inferred from transcriptome-wide sequencing of RNA 5′ ends (*23*–*25*). (**F**) Folding energy of RNA termini predicted by term-seq (n = 1443 sites, green bars) compared with random intergenic sites (n = 10,000 sites, red bars). (**G**) Uridine-rich tail upstream to term-seq sites (n = 1443 sites).

detected regulate genes of diverse functions, including some involved in virulence. For example, deletion of the conditional-termination regulator of *lmo0559*, called *rli31* (Fig. 2F), led to an attenuated virulence phenotype of *L. monocytogenes* in mouse and butterfly infection models (*37*). Deletion of *rli31* also led to decreased lysozyme resistance of *L. monocytogenes* in blood (*38*). These results imply that the termination-based regulatory elements we detected may control multiple physiological- and pathogenicity-relevant processes.

Genome-wide metabolite screening in physiological conditions

Although our data uncover multiple cases of new candidate regulators, they do not reveal the metabolites to which these regulators respond. Discovery of the metabolite that controls the activity of a given candidate regulator is a major challenge in the field and usually involves in vitro structural probing of the regulator in the presence of various candidate metabolites and/or the construction of reporter assays to monitor the activity of the regulator (*1*–*3*).

We developed a term-seq–based strategy to evaluate multiple possible metabolites across all candidate regulators simultaneously in physiological, in vivo conditions. We reasoned that the presence of the metabolite should alter the open/closed state

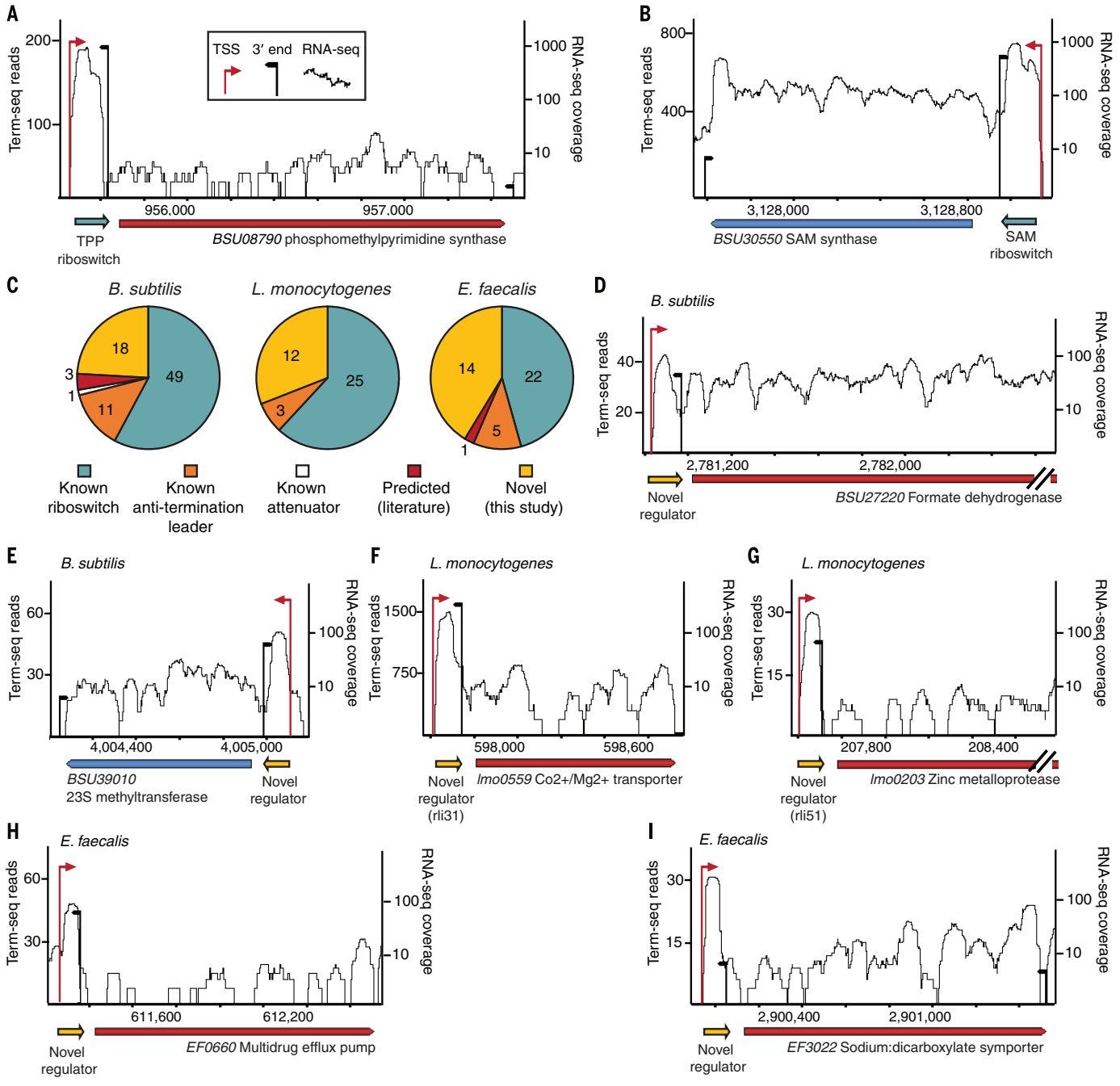

Fig. 2. Discovery of genes regulated by conditional termination. Known riboswitches in *B. subtilis* display a typical pattern of premature termination in the 5′UTR. In both (**A**) thiamine pyrophosphate (TPP) riboswitch and (**B**) lysine riboswitch (blue arrows), a term-seq site is observed downstream to the riboswitch. (**C**) Known and previously unidentified regulators identified by applying term-seq on *B. subtilis*, *L. monocytogenes*, and *E. faecalis*. Pie charts indicate the number of regulators identified in each functional category and organism (tables S2 to S5). (**D** to **I**) Examples of previously unidentified regulatory elements (yellow arrows) identified in this study. Axes and colors are as in Fig. 1E.

of the regulator and that this state can be quantitatively measured as the ratio between the full-length RNA and the short, prematurely terminated form (Fig. 3A). Because term-seq directly provides a read-through measure (quantification of short/long transcript ratios) for every expressed regulator in the genome, it enables low-cost, parallel analysis of in vivo regulator activities following the application of any metabolite of interest.

To validate this approach, we grew *B. subtilis* in a defined medium with or without the amino acid lysine. Out of the 82 regulators mapped in *B. subtilis*, only the two known lysine riboswitches showed a considerable increase in read-through levels as a result of lysine depletion (Fig. 3, B and C, and fig. S4). Moreover, depletion of a different amino acid from the medium (methionine) (Fig. 3, B and C) did not increase the open/closed ratio of the lysine riboswitches, pointing to high specificity in sensing the presence of lysine.

Antibiotic-controlled conditional termination regulates antibiotic resistance genes

Because inducible antibiotic resistance mechanisms pose a major medical challenge, we screened for regulators that respond to the presence of antibiotics. The rRNA methylase gene *ermK* confers resistance to macrolide-lincosamide-streptogramin B antibiotics and is controlled by conditional premature termination that is alleviated when the antibiotic is introduced (*39*). Reports have described similar regulation in additional antibiotics resistance genes, but this mode of regulation was considered rare (*30*, *32*). We thus searched for antibiotic-responsive regulators by applying term-seq to *B. subtilis*, *L. monocytogenes*, and *E. faecalis* after short exposure to sublethal doses of seven different antibiotics (table S6) (*23*). Six of the regulators we identified (tables S2 to S5) showed an antibiotic-dependent response, characterized by read-through into the downstream gene in the presence of the antibiotic (Fig. 4 and fig. S5).

Two antibiotic-responsive, termination-based regulatory elements were observed in each of the three bacteria studied. In *B. subtilis*, we identified the *vmlR* (*32*) and *bmrB* (*30*) regulators, which regulate the expression of antibiotic resistance genes through an unknown or ribosome-mediated mechanism, respectively (Fig. 4, A and B). In *L. monocytogenes*, however, we discovered two new regulators that were previously annotated as conserved *Listeria* small RNAs (sRNAs) of unknown function, *rli53* and *rli59*, and were hypothesized to act in cis (*36*). We found that these two sRNAs function as antibiotic-responsive riboregulators that control the expression of the genes *lmo0919* and *lmo1652*, both encoding ABC transporter genes of unknown function (Fig. 4, C and D). Whereas the alteration in the open/closed state of *lmo0919* by *rli53* was highly specific to lincomycin, *rli59* was more permissive and responded to several different translation-inhibiting antibiotics (Fig. 4, C and G). In *E. faecalis*, it was previously shown that expression of the *msrC* macrolide-resistance efflux pump increases in response to erythromycin exposure (*40*). Our data suggest that the *msrC* response results from a coordinated activity of its promoter and a previously unidentified termination-based regulator, which, upon exposure to the antibiotic, act in concert to increase both the transcription initiation rate (7.3-fold) and read-through into the gene (4.6-fold) (Fig. 4, E and G). We detected a similar promoter termination–synchronized activity for the *B. subtilis vmlR* gene (Fig. 4B). Last, we found an additional lincomycin-specific

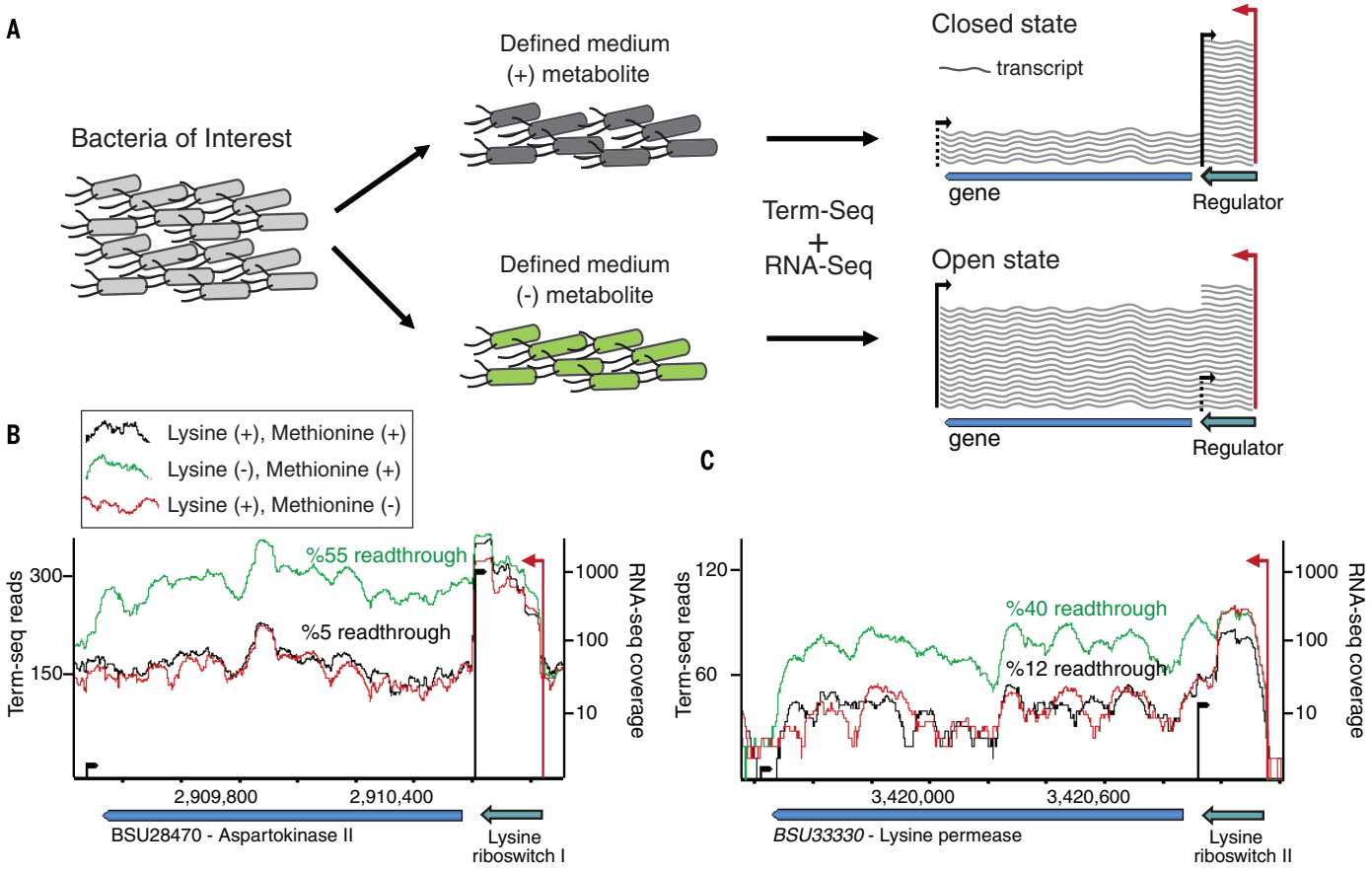

Fig. 3. In vivo metabolite screening by using RNA sequencing. (**A**) Genome-wide experimental approach for in vivo screening of termination-based regulators that respond to a metabolite of choice in physiological conditions. A bacterium of interest is cultured in a defined medium with or without the metabolite of choice. After a brief incubation, RNA is extracted and sequenced by using term-seq and RNA-seq. The long/short transcript ratio, indicative of the open/closed state of the regulator, can be calculated from term-seq or RNA-seq counts. (**B** and **C**) *B. subtilis* was grown in defined, minimal media either containing both lysine and methionine (black RNA-seq coverage), lacking lysine and containing methionine (green), or containing lysine and lacking methionine (red). RNA-seq coverage was normalized by the number of uniquely mapped reads in each sequencing library.

termination-based regulator that controls the expression of yet another ABC transporter of unknown function, *EF2720*, in *E. faecalis* (Fig. 4F).

The presence of antibiotic-responsive, termination-based regulatory elements upstream of specific genes in *L. monocytogenes* and *E. faecalis* suggest that these are possible, previously unknown antibiotic resistance genes. We further characterized the antibiotic-based regulation of *lmo0919*, an ABC transporter of unknown function in *L. monocytogenes*. This gene was previously suggested to be involved in antibiotic resistance on the basis of its distant homology to the staphylococcal *Vga* gene and its heterologous activity in staphylococcal hosts (*41*), but its function in *L. monocytogenes* remained unknown. We found that deletion of *lmo0919* rendered *L. monocytogenes* fourfold more sensitive to the antibiotic lincomycin but did not reduce the minimum inhibitory concentration (MIC) of other antibiotic classes (table S7). The protein encoded by *lmo0919* therefore confers lincomycin-specific antibiotic resistance, which is consistent with the specific activation of its 5′UTR regulator by lincomycin but not by erythromycin or chloramphenicol (Fig. 4, D and G).

The mechanism of antibiotics-mediated conditional termination in *lmo0919*

Inspection of the regulatory 5′UTR sequence of *lmo0919* revealed a potential two-stem, terminator/antiterminator structure (Fig. 5A). Such structures are common in riboswitches and attenuators and can adopt two alternative conformations: one that

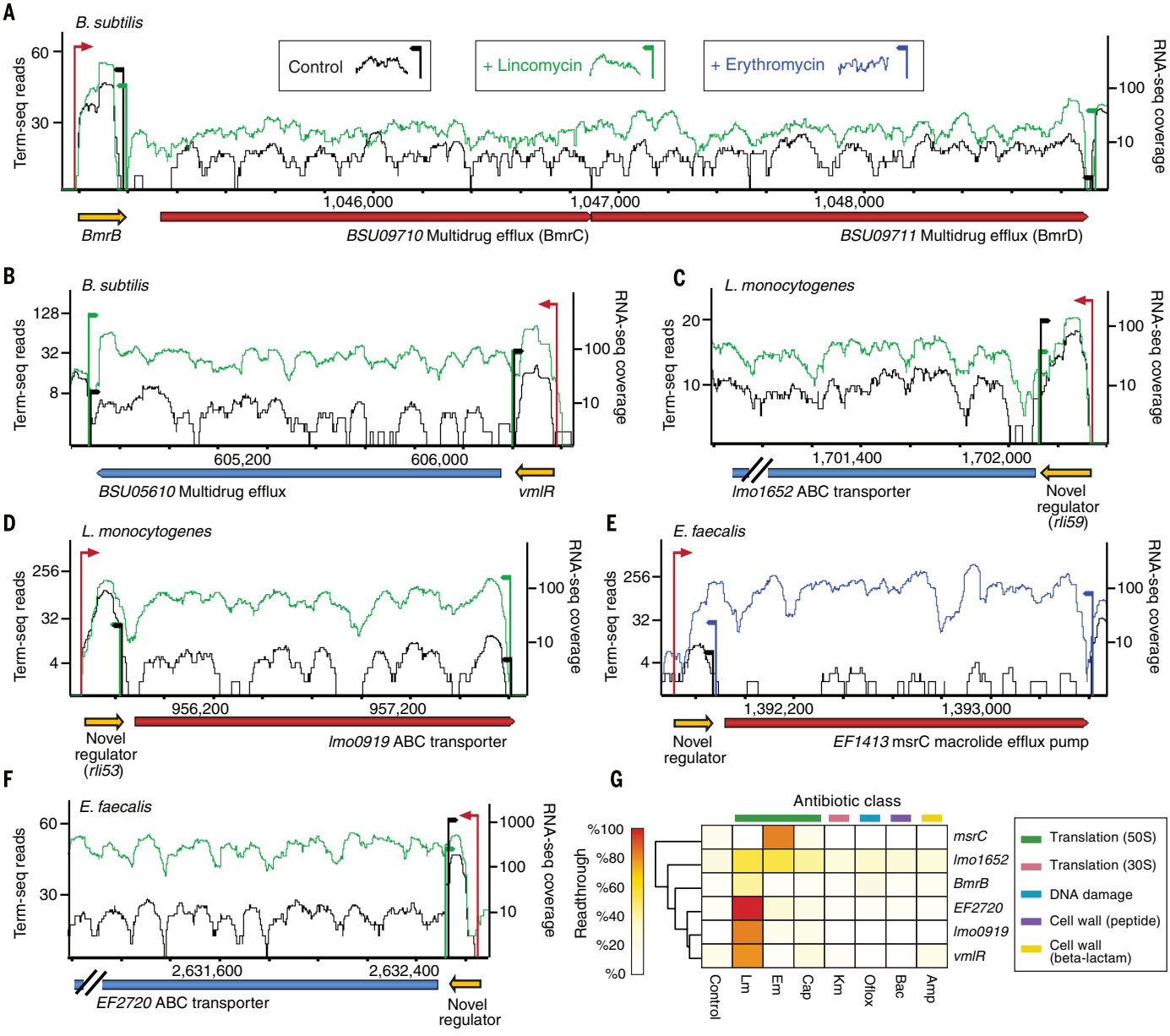

Fig. 4. Antibiotic-responsive conditional terminators. The antibiotic-dependent response of known and previously unidentified regulators as measured in vivo by means of term-seq and RNA-seq. Black, green, and blue RNA-seq coverage and term-seq sites denote the control (LB), lincomycin, and erythromycin conditions, respectively. Term-seq sites represent average read coverage across three biological replicates. (**A**) The *B. subtilis bmrCD* operon. (**B**) The *B. subtilis vmlR* gene. (**C** to **F**) Antibiotic dependent transcriptional read-through in previously unidentified regulators discovered in *L. monocytogenes* and *E. faecalis*. (**G**) Condition-specific read-through calculated in the control and the seven antibiotics exposure experiments. The antibiotic class is defined by the cellular process/component targeted. RNA-seq was normalized as in Fig. 3. Lm, lincomycin; Em, erythromycin; Cap, chloramphenicol; Km, kanamycin; Oflox, ofloxacin; Bac, bacitracin; and Amp, ampicillin.

generates a transcriptional terminator (Fig. 5A, left), and another in which the antiterminator promotes transcriptional read-through by interfering with terminator formation (Fig. 5A, right). To enquire whether this mode of regulation occurs in the case of *lmo0919*, we engineered mutations in either the first or the second arm of the first stem, disrupting the putative anti-antiterminator or the antiterminator, respectively

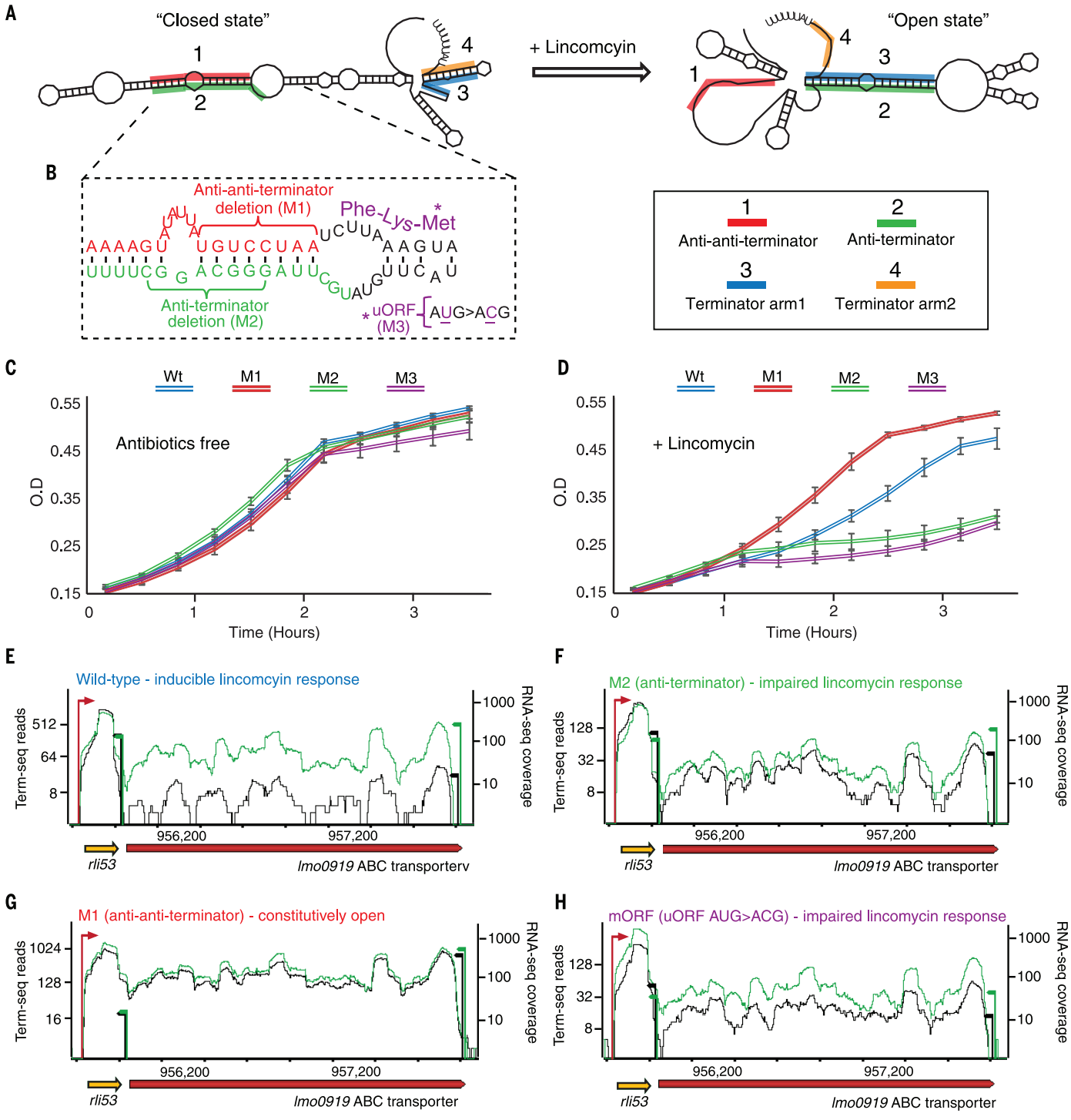

Fig. 5. Antibiotic-responsive terminator/antiterminator RNA structures control the expression of *lmo0919*. Mutational analysis of the 5′UTR of *lmo0919* provides insights into the mechanism of inducible antibiotic resistance. (**A**) A predicted RNA secondary structure of the *lmo0919* 5′UTR. This element is predicted to form two alternative, mutually exclusive structures that mediate either termination or antibiotic-dependent read-through. (Left) The "closed-state" structure encodes a terminator and an upstream stem. (Right) The "open-state" structure in which the terminator structure is sequestered by an antiterminator. (**B**) Generation of mutants that interrupt the anti-antiterminator (red), the antiterminator (green), or a conserved uORF that overlaps the anti-antiterminator (purple). (**C** and **D**). Mutants were grown in BHI media without lincomycin (C) or containing 0.5 μg/ml lincomycin (D), respectively. Error bars represent standard error. (**E** to **H**) Term-seq and RNA-seq coverage of wild-type and mutants grown in BHI without lincomycin (black RNA-seq curves and black term-seq sites) or with 0.5 μg/ml lincomycin (green RNA-seq curves and green term-seq sites). RNA-seq coverage was normalized as in Fig. 3.

(Fig. 5B). Consistent with the model, deletion of eight nucleotides from the antiterminator kept the regulator in a constitutively "closed" state, even in the presence of lincomycin antibiotic, rendering the bacteria sensitive (Fig. 5, B to E and F, and table S8). In contrast, deletion of eight nucleotides from the anti-antiterminator freed the antiterminator to interfere with the terminator structure, leading to constitutive read-through ("open" state), even in the absence of antibiotics, and resulting in increased resistance to lincomycin (Fig. 5, B to E and G). These results support a model in which the lincomycin-dependent activation of *lmo0919* expression is mediated by a structural interplay of terminator/antiterminator structures in the 5′UTR of this gene.

The structural alterations in the *lmo0919* ribo-regulator could either be mediated by direct binding of the antibiotic to the ribo-regulator (a riboswitch), or by attenuation, in which the lincomycin-inhibited ribosomes stall on an uORF in the ribo-regulator, thus shifting the ribo-regulator structure from a "closed" to an "open" state (as suggested for the *bmrB* regulator in *B. subtilis*) (*30*). To differentiate between these mechanisms, we measured the lincomycin-dependent induction of *lmo0919* in *L. monocytogenes* expressing the ErmC 23*S* rRNA methyltransferase (*23*, *42*). In these bacteria, the ribosomes are dimethylated at position A2058 of the 23*S* rRNA, rendering the ribosomes resistant to lincomycin (*42*). In ErmC-expressing bacteria, the *lmo0919* regulator was no longer responsive to lincomycin (fig. S6), suggesting that this ribo-regulator depends on stalled ribosomes for its activity and does not interact directly with the antibiotic molecule.

We then performed a comparative analysis of the 5′UTR sequences of *lmo0919* homologs in various Gram-positive bacteria (*23*). Although the nucleotide sequence of the ribo-regulator showed almost no conservation between species, the terminator/antiterminator architecture was strictly conserved among all homologs (figs. S7 and S8). Despite the near lack of sequence conservation, all

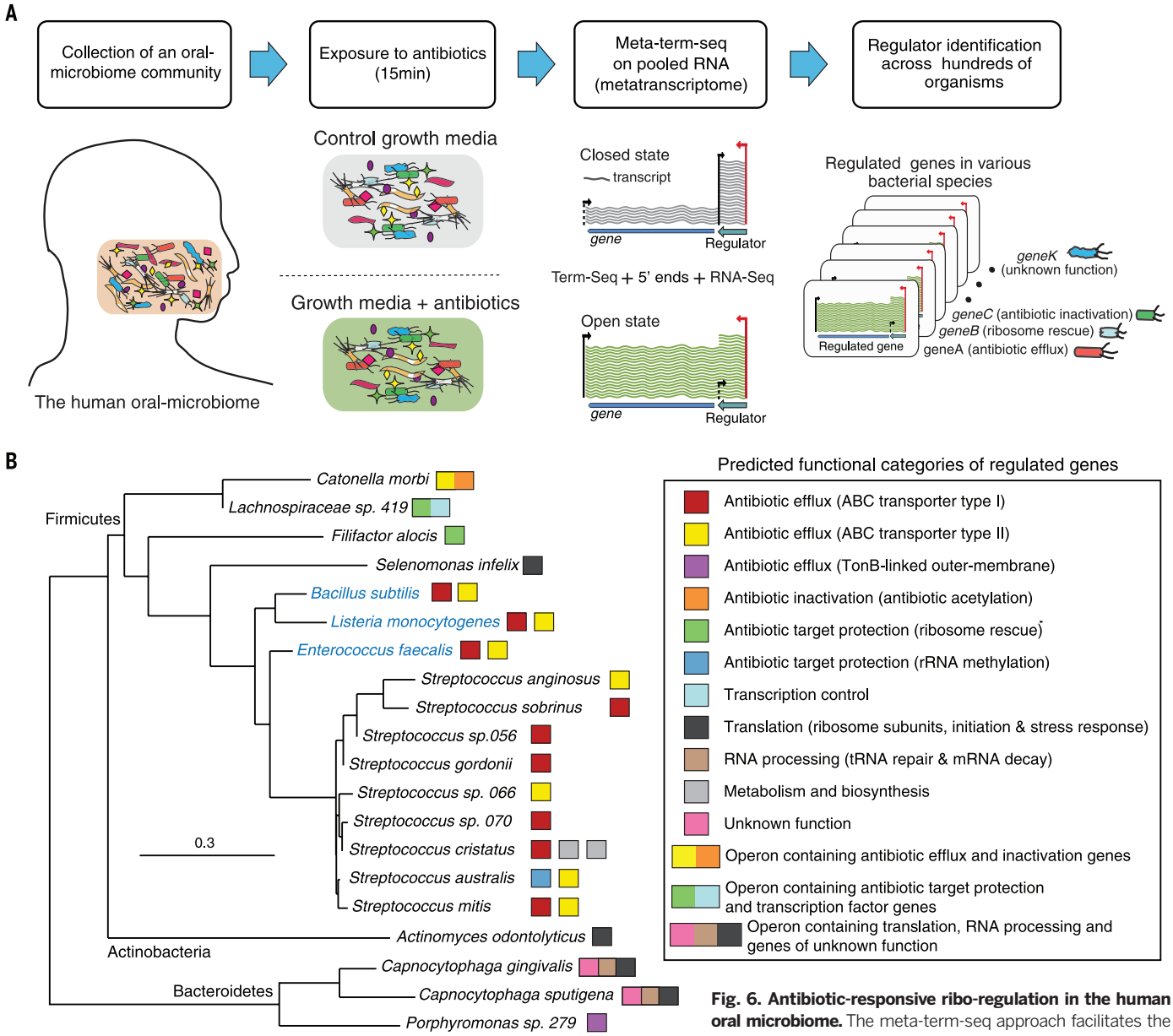

Fig. 6. Antibiotic-responsive ribo-regulation in the human oral microbiome. The meta-term-seq approach facilitates the discovery of metabolite-responsive regulators across complex bacterial communities. (**A**) Schematics of the meta-term-seq workflow, from sample collection to regulator identification. (**B**) A 16*S* rRNA phylogenetic tree comprising oral microbiome bacteria found to have one or more lincomycin-responsive regulators (*23*). The predicted functions of the regulated genes in each species are indicated with colored boxes according to the inset legend. In some cases, a single operon contained several different functions (multicolored rectangles, legend bottom). Individual bacteria studied in monoculture were added to the tree (marked with blue-colored names).

regulators contained a three-amino-acid uORF exactly overlapping the inhibitory anti-antiterminator sequence (Fig. 5B and figs. S7 and S8). Although such small ORFs were never previously reported to be involved in transcriptional attenuation, the strong positional conservation of the uORF in the ribo-regulator led to the hypothesis that its translation forms the basis for the attenuation-based regulation. Indeed, a green fluorescent protein (GFP) fusion assay showed that this uORF is translated in *L. monocytogenes* in vivo (fig. S9) (*23*).

To characterize the effects of lincomycin on the interaction between the ribo-regulator and the ribosome, we measured the levels of ribosome occupancy over the ribo-regulator in control and lincomycin-treated bacteria using ribosome profiling (Ribo-seq) (*23*, *43*). We detected approximately five- and twofold increases in ribosome occupancy over the three-amino-acid uORFs in *L. monocytogenes* and *Listeria innocua*, respectively, after brief exposure to lincomycin (fig. S10) (*23*). These results show that lincomycin-inhibited ribosomes specifically stall at the three-amino-acid uORF that overlaps the anti-antiterminator sequence.

Collectively, these results point to an attenuation-based regulatory mechanism in which the association of the ribosome with the antibiotic leads the ribosome to stall on a nine-base uORF that overlaps the anti-antiterminator, releasing the antiterminator to interfere with terminator folding and thus allowing read-through into the antibiotic resistance gene. Indeed, a single-base mutation that changed the ATG (Met) initiation codon of the uORF into ACG led to suppressed lincomycin-dependent read-through, validating the model (Fig. 5, B, D, and H).

The *lmo0919* regulator is specifically activated by lincomycin but not by erythromycin (Fig. 4), although both antibiotics induce ribosome stalling. Although antibiotics of the lincomycin family inhibit ribosome progression after the incorporation of one to two amino acids, erythromycin requires the addition of six to eight amino acids to the nascent chain before it stalls the ribosome (*44*). It is therefore possible that the specificity of the *lmo0919* ribo-regulator to lincomycin stems from the short size of its functional uORF.

Abundance of antibiotic-dependent ribo-regulation in the human microbiome

The presence of multiple antibiotic-responsive, termination-based regulatory elements in three evolutionary distant bacterial species prompted us to hypothesize that this mode of regulation is commonly controlling antibiotic resistance in nature. We thus probed for such regulatory elements in the human oral microbiome, a complex microbial community comprising hundreds of commensal teeth- and mouth-associated bacterial species that are frequently naturally exposed to antibiotics (*45*).

We used a meta-transcriptomics approach (denoted here "meta-term-seq") in order to probe the transcriptional profile of the microbial consortium in a single experiment. For this, teeth-associated bacteria were sampled from three healthy individuals and were pooled in tubes containing brain heart infusion (BHI) medium with and without the antibiotic lincomycin for 15 min. We applied term-seq and RNA-seq on pooled RNA and mapped RNA reads to the >400 reference genomes from the human oral microbiome project (*23*, *45*, *46*). We further studied the antibiotic-responsive meta-term-seq profiles in the 167 species that showed considerable expression of at least 10% of their genes (*23*).

Operons activated by alleviation of premature termination in response to lincomycin were abundantly found in members of the human oral microbiome. We detected 21 regulatory elements, overall controlling 57 genes, in which transcriptional read-through was substantially increased after the application of lincomycin (Fig. 6, fig. S11, and tables S1 and S8) (*23*). Such elements were detected in 21% (13 of 61) of the Firmicutes studied, indicating that this mode of regulation is common in bacteria in this phylum. The genes regulated by the antibiotic-responsive cis-acting RNA elements included several different classes of multidrug antibiotics exporters and efflux pumps (*47*, *48*), rRNA methylases known to confer antibiotic resistance via modification of the ribosomal RNA (*39*), acetyltransferases known to directly deactivate the antibiotic via acetylation (*49*), genes annotated as tetracycline resistance small-guanosine triphosphatases that rescue antibiotic-bound ribosomes (*50*), and additional genes that have no described antibiotic resistance (Fig. 6, fig. S11, and tables S1 and S8). These results highlight meta-term-seq as a method with which to probe gene regulation in microbial consortia and reveal a common control mechanism for antibiotic-resistance genes in human-associated bacteria.

Discussion

We present here an unbiased experimental method for high-throughput discovery of conditional termination–based regulators in individual bacteria as well as in microbiomes. Moreover, we developed a screening procedure that measures the in vivo read-through levels of every regulator in the genome in parallel, thus enabling the identification of regulators that specifically respond to a given metabolite. By screening for ribo-regulators that respond to antibiotic molecules, we highlight a common form of regulation of antibiotics resistance genes and expose the molecular details entailing its mechanism of action.

Through the use of term-seq, which does not rely on comparative genomics, we overcome the challenge of identifying highly divergent or evolutionarily new regulators, as well as short regulators, both of which are generally challenging or even impossible to find when relying on sequence conservation (*19*). Furthermore, with the ability of term-seq to measure the in vivo activity of every expressed regulator in the cell in parallel, we prevent experimental biases that stem from artificial transfer of the regulator to a model organism and allow for large-scale screens and studies of regulators in organisms that lack genetic engineering tools. In addition, our meta-term-seq approach enables parallel discovery of ribo-regulators in multiple organisms belonging to a bacterial consortium, even if these organisms are noncultivated. Nevertheless, although our approach identifies metabolite-responsive regulators, it does not differentiate between riboswitches, attenuators, and protein-dependent termination and moreover cannot identify riboswitches and attenuators functioning via translation inhibition rather than premature termination. Our approach will also work only for metabolites that can enter the cell (for direct binding to riboswitches) or can be sensed by the cell. Last, another limitation of the approach is that the read-through response we record in the regulator may be due to a metabolite different than the one added in the screen. This would occur, for example, when the added metabolite leads to changes in the levels of the true metabolite. However, because the riboswitch-mediated response is direct and hence expected to be very rapid, these secondary effects could be mitigated if the exposure to the screened-for metabolite is very short, as done in our antibiotic-exposure experiments.

Termination-based regulation of antibiotic resistance genes have so far been sporadically described (*30*, *32*, *39*). Our identification of numerous regulators in model organisms and in many species of the human oral microbiome indicates that such regulation of antibiotic resistance genes is very common in Gram-positive bacteria. Moreover, even in the three model organisms that we studied in depth, additional antibiotic-dependent regulators may be present. For example, in *B. subtilis* we identified a previously unknown regulator upstream to *BSU39010* (Fig. 2E). In *Streptomyces fradiae*, this gene methylates the 23*S* rRNA at position G748, which was shown to provide a highly specific resistance to the macrolide antibiotic tylosin, but not to other macrolides. (*51*). Although we did not observe an antibiotic-dependent response in this regulator, it is conceivable that it would show a specific response to tylosin, which was not included in our screen. In addition, regulators were found for the *L. monocytogenes lmo2760* and the *E. faecalis EF0660* genes (Fig. 2H), both of which are homologous to multidrug efflux pumps. These regulators possibly respond to antibiotics other than the ones we used in our screen.

The importance of termination-based cis-regulators in maintaining the versatile physiology of bacteria is evident from their nearly ubiquitous distribution across the bacterial kingdom (*33*). We now provide the tools with which we can identify and characterize many of these in the future.

Materials and methods

Oligonucleotides, wild-type bacterial strains, and culture conditions

All oligonucleotides used in this study were purchased from Sigma (St. Louis, Missouri) or Integrated DNA Technologies (IDT, San Jose, California) (table S9). *Bacillus subtilis* str. 168, *Listeria monocytogenes* EGDe, *Listeria innocua* Clip11262, and *Enterococcus faecalis* ATCC 29212 were cultured under aerobic conditions at 37°C with shaking in either LB (10 g/L tryptone, 5 g/L yeast extract 5 g/L NaCl), TB (12 g/L tryptone, 24 g/L yeast extract, 0.4% glycerol, 2.2 g/L KH_2PO_4 and 9.4 g/L K_2HPO_4),

BHI broth (Difco, Franklin Lakes, New Jersey), or M9 minimal media [0.5% w/v glucose, 2 g/L $[NH4]_2SO_4$, 18.3 g/L K2 $HPO_4 \cdot 3H_2O$, 6 g/L $KH2PO_4$, 1 g/L sodium citrate, 0.2 g/L $MgSO_4 \cdot 7H_2O$, 5μM $MnCl_2$, and 5μM $CaCl_2$, tryptophan (Sigma) 50μg/mL].

Lysine-responsive regulation

B. subtilis was grown overnight in LB and then diluted 1:200 into 150 ml of M9 media supplemented with lysine and methionine (50μg/mL each). Bacteria were grown to OD_{600} = 0.9 to 1.0, washed, and then resuspended to an OD_{600} = 0.3 in 3 ml of M9 media, containing the following combinations of amino acids at a final concentration of 50 μg/mL: lysine and methionine (lys^+ met^+), methionine only (lys^- met^+), or lysine only (lys^+ met^-). Cells were incubated for 2 hours and collected by means of centrifugation (4000 rpm, 5 min, and 4°C) followed by flash freezing. Samples were stored in −80°C until RNA extraction.

Antibiotics-responsive regulators

A sublethal concentration for the antibiotics lincomycin, erythromycin, chloramphenicol, kanamycin, ofloxacin, ampicilin, and bacitracin (Sigma) was determined for each of the organisms used in this study as follows. Bacterial cultures were propagated in LB or BHI overnight in triplicates and diluted 1:200 into fresh media. Cultures were grown to early exponential phase (OD_{600} = 0.1 to 0.2) and then supplemented with serially diluted antibiotics stocks. The growth rate was dynamically monitored in intervals of 10 to 15 min by using a 96-well plate format optical density (OD) reader (Infinite M200 Tecan) for a period of at least 4 hours. The highest antibiotics concentration that did not cause growth-rate inhibition as compared with the no-antibiotics control was chosen as the sublethal dosage (table S7). To identify antibiotic-responsive regulators, bacteria were grown in LB or BHI in triplicates as described above and, upon reaching early exponential phase, 5-ml cultures were independently exposed for 15 min to the sublethal concentration of each antibiotic as determined above. Bacteria were then collected by means of centrifugation, flash frozen, and stored in −80°C until RNA extraction.

RNA isolation

Frozen bacterial pellets were lysed by using the Fastprep homogenizer (MP Biomedicals, Santa Ana, California), and RNA was extracted with the FastRNA PRO blue kit (MP Biomedicals, 116025050) according to the manufacturer's instructions. RNA levels and integrity were determined with Qubit RNA BR Assay Kit (Life technologies, Carlsbad, California, Q10210) and Tapestation (Agilent, Santa Clara, California, 5067-5576), respectively. All RNA samples were treated with TURBO deoxyribonuclease (DNase) (Life technologies, AM2238).

Construction of mutated Listeria strains

For mutant generation with pMAD-based plasmids (*52*), ~600 nucleotide (nt) regions of complementarity both upstream and downstream of a targeted region were either ordered as gBlocks (IDT) and amplified with gBlock-Up and -Down oligonucleotides (table S9) complementary to uniform flanks on each gBlock corresponding to the 40 nt on either side of the pMAD multicloning site, or polymerase chain reaction (PCR) amplified with Phusion High fidelity polymerase and reagents (Finnzymes, F-553) by using genomic DNA as a template and then joined by a second splice overlap extension PCR reaction by using the first two PCR products as template to generate an Upstream-Downstream (UD) PCR product (table S9, *lmo0919* deletion). PCR products were subsequently purified with QIAquick PCR purification columns (Qiagen, Hilden, Germany, 28104), digested with the SalI and XmaI restriction enzymes [New England BioLabs (NEB), Ipswich, Massachusetts], purified again as before, and ligated into SalI/XmaI digested pMAD plasmid for 1 hour at 25°C with T4 DNA ligase (NEB, M0202S). Two microliters of each ligation were transformed into chemically competent *Escherichia coli* Top10 (Invitrogen, Carlsbad, California, C404003) cells according to the manufacturer's instructions. Transformants were screened by means of PCR and Sanger sequencing for the presence of the appropriate insert. Electrocompetent *L. monocytogenes* strains were transformed with the respective plasmid and mutagenesis carried out as described previously (*52*). Briefly, after transformation and plating onto selective BHI, 5 μg/ml erythromycin (Em) 80 μg/ml 5-bromo-4-chloro-3-indolyl-β-D-galactopyranoside (X-gal) plates, bacteria were grown at 30°C for 2 days. A single blue colony was picked and transferred to liquid BHI broth and grown for an additional 6 hours at 30°C. The colony was then diluted 1:1000 into 10 ml of BHI-Em and grown overnight at 42°C, which prevents pMAD replication in the cytosol owing to a temperature-sensitive ori. Serial dilutions were plated onto BHI-X-gal-Em plates and grown for 2 days at 42°C, and the process was reiterated several times until white colonies, in which the plasmid integrated into the genome, were recovered. Colonies were screened by means of colony PCR, and mutants were confirmed with Sanger sequencing.

For the construction of the GFP reporter strain, a translational fusion was constructed by generating a synthetic 1936–base pair (bp) fragment (*rli53*-GFP) encompassing the upstream region of *rli53* (591 bp), the 5′ of rli53 (40 bp) and a small spacer (30 nt) fused to the GFP optimized for *Listeria* (*53*) that lacks the initiator codon and followed by the downstream region of *rli53* (549 bp) (IDT) (table S9). The construction was cloned into the BamHI and EcoRI restriction sites of the suicide vector pMAD (*52*) in order to generate the plasmid pMAD-rli53-GFP used to transform the wild-type strain *L. monocytogenes* EGD-e as described above, and generating the *L. monocytogenes* strain expressing the chromosomic fusion *rli53*-GFP. The sequence was verified with DNA sequencing by using primer oligonucleotides (*lmo0918*-upstream and *lmo0919*-downstream) (table S9).

MIC determination

The MIC was determined in broth culturing conditions in the presence of serially diluted antibiotic concentrations. Briefly, the bacterial strains were grown overnight at 37°C in BHI agarose plates, and 1 to 3 single colonies were collected into 1 ml of BHI broth. The OD_{600} was adjusted to 0.01 and then diluted 1:10 into a 96-well plate containing a final volume of 200 μl BHI supplemented with twofold serial dilutions of lincomycin, erythromycin, and chloramphenicol. The samples were grown over 2 days at 37°C without shaking, and the MIC was determined as the lowest antibiotic concentration to fully inhibit growth.

Term-seq library preparation

DNAse-treated RNA (1 to 5 μg) was subjected to a 3′ end–specific ligation by mixing 5 μl of RNA solution with 1 μl of a 150 μM DNA adapter solution (table S9), 2.5 μl of 10X T4 RNA ligase1 buffer, 2.5 μl of 10 mM adenosine triphosphate, 2 μl of dimethyl sulfoxide, 9.5 μl 50% PEG8000, and 2.5 μl of T4 RNA ligase1 enzyme (NEB, M0204). The reaction was incubated for 2.5 hours at 23°C and then cleaned by adding 2.2× (55 μl) paramagnetic SPRI beads (Agencourt AMPure XP, Beckman Coulter, Brea, California), mixing well by pipetting and leaving the reaction-bead solution to rest at room temperature for 2 min. The supernatant was separated from the beads by using a 96-well magnetic separator (Invitrogen). Beads were washed on magnet (beads securely attached) by discarding the solution and adding 120 μl of 70% ethanol (EtOH), allowing an incubation period of 1 min. The cleanup stage was repeated, and the beads were air dried for 5 min. The RNA was eluted in 5 to 10 μl of H_2O. The RNA was fragmented with fragmentation buffer (Ambion) in 72°C for 1.5 min. The fragmentation reaction was cleaned by using SPRI beads 2.2× as described above and eluted in 28 μl of H_2O. Ribosomal RNA was depleted by using the Ribo-Zero rRNA Removal Kit (epicenter, MRZB12424) or MICROBExpress (Life technologies, AM1905) according to the manufacturer's instructions. Depleted RNA was reverse transcribed by incubating 11 μl of RNA with 1 μl of 10μM reverse transcription primer (table S9), incubating at 65°C for 5 min, and immediately placing on ice for 2 min. Two microliters of AffinityScript reverse transcriptase (Agilent, 600559), 2 μl of 10X Affinity Script Buffer, 2 μl of 100 mM DTT, and 2 μl of 10 mM deoxynucleotide triphosphates (Sigma, D7295) were added, and the reaction was incubated at 42°C for 45 min and then terminated by incubation at 75°C for 15 min. To degrade the RNA template, 1 μl of ribonuclease (RNase) H (NEB, M0297) was added, and the reaction was incubated for an additional 30 min at 37°C. The reaction was cleaned by using SPRI beads at a 2.2× ratio (46 μl) and eluted in 5.5 μl of H_2O. Five microliters of the resulting cDNA was subjected to a second 3′ end ligation, as above, but using a cDNA-specific ligation adapter (table S9). The reaction was incubated at 23°C for 4 to 8 hours and then cleaned with SPRI beads at a 1.8× ratio (45 μl), eluting the cDNA in 23 μl of H_2O. Twenty-two microliters of ligated cDNA solution was mixed with 1.5 μl of forward and reverse primers, at 25 μM each (table S9) and 25 μl of KAPA Hi-Fi PCR-ready mix (KAPA Biosystems,

Wilmington, Massachusetts, KK2601). The library was amplified by using the manufacturer's protocol with 16 to 18 amplification cycles. The final term-seq library was cleaned with SPRI beads at a 0.9× ratio (45 μl), and the concentration and size distribution were determined with the Qubit dsDNA BR Assay Kit (Life technologies, Q32850) and the dsDNA D1000 Tapestation kit (Agilent, 5067-5582), respectively.

RNA-seq and 5′ end sequencing

For RNA-seq library preparation, 4 μg of DNase-treated RNA was fragmented in 20 μL of reaction volume as described above and cleaned by adding 2.5× (50 μl) SPRI beads and 30% v/v isopropanol (30 μl). The beads were washed with 120 μl of 80% EtOH and then air dried as described above. The RNA was eluted in 26 μl of H_2O, and rRNA was depleted as in term-seq. Strand-specific RNA-seq was performed with the NEBNext Ultra Directional RNA Library Prep Kit (NEB, E7420) with the following adjustments to the manufacturer's instructions: All cleaning steps were carried out with 2.5× SPRI beads and 30% v/v isopropanol combinations, the washing steps were performed with 450 μl of 80% EtOH, and only one cleanup step was performed after the end repair step. The resulting libraries concentrations and sizes were evaluated as in term-seq. For 5′ end sequencing, the RNA was divided into a tobacco acid pyrophosphatase (TAP)–treated and untreated (noTAP) reactions, which were subsequently sequenced by using a 5′ end–specific library preparation protocol described in (*25*). In *B. subtilis*, the 5′ end libraries were prepared with bacteria grown to early exponential phase in TB medium. For *L. monocytogenes*, 5′ end data was taken from (*25*).

Deep-sequencing, read mapping, and counting

RNA-seq, 5′end, and term-seq libraries generated in this study (table S10) were sequenced by using the Illumina Miseq, HiSeq. 1500, or NextSeq. 500 platforms. Sequenced reads were demultiplexed, and adapters were trimmed by using Casava v1.8.2. Reads were mapped to the reference genomes (Gene annotation and sequences were downloaded from GenBank: AL009126, NC_003210, and NC_003212 NC_004668 for *Bacillus subtilis* str. 168, *Listeria monocytogenes* EGD-e, *Listeria innocua* Clip11262, and *Enterococcus faecalis* V583, respectively) by using NovoAlign (Novocraft) v3.02.02 with default parameters, discarding reads that were nonuniquely mapped as previously described in (*25*). All downstream analyses were performed by using custom written perl and R scripts (available through GitHub under repository aad9822).

RNA-seq–mapped reads were used to generate genome-wide RNA-seq coverage maps. 5′ end and term-seq positions were determined as the first nucleotide position of the mapped read. Total 5′ end or term-seq coverage was calculated per nucleotide position in the genome. The data was visualized by using a custom browser as described in (*25*) (Figs. 1 to 5). TSSs were determined as in (*25*). Briefly, the ratio between TAP-treated (TAP) and untreated (noTAP) was calculated for each genomic position covered by least four reads in the TAP condition. The maximal 5′UTR allowed was set to 450 nt, and the TSS was chosen as the site with a TAP/noTAP ratio greater than 2 for *B. subtilis* and greater than 1 for *L. monocytogenes* and *E. faecalis*. In cases in which multiple potential TSSs were available, the site with the highest coverage was chosen as the gene TSS.

Terminator identification and analysis

For the assignment of terminators to genes, the downstream sequence of each gene (up to 150 nt, allowing up to 10 nt invasion to the next gene) was scanned for term-seq sites that were covered by a minimum of four reads in each of the three biological replicates. In case multiple sites were observed, the site with the highest coverage was selected as the terminator. This filtering resulted in 84.4% (±0.7%) of the reads mapping to noncoding positions, representing >50-fold enrichment over what would have been expected by chance based on the coding:noncoding composition of the *B. subtilis* genome ($P = 0$, binomial exact test). For terminator sequence and structure analysis, the 40-nt upstream and 20-nt downstream sequences were collected for each terminator and folded in silico via the RNAfold software by using the standard parameters (*54*). For 96% (1382 of 1443) of the sites we predicted as terminators, there was a clear stem/loop structure preceding the site, with 91% (1302 of 1443) of them preceded by at least four uridine residues in the eight bases immediately upstream to the termination position, which is in agreement with the known features of Rho-independent terminators (table S2 and fig. S1). Nucleotide logos were generated by using WebLogo (*55*)

Previously established terminators inferred by experimental assays such as Northern blots or S1 nuclease mapping of the 3′ end (*56*) were collected for *B. subtilis* genes covered by at least 25 RPKM RNA-seq reads (table S11) and then compared with the term-seq–inferred terminator set described in table S1. We were able to detect 43 of 46 (93%) known, high-confidence terminators (table S11). Two of the three terminators that were not detected with term-seq were associated with genes of relatively low expression (76 and 90 reads per million per kilobase), which could explain why they did not appear with a sufficient number of reads in the three biological repeats to be considered by our filtering criteria.

Discovery of premature termination

For the discovery of premature termination, the 5′UTR (the beginning of which was defined by the TSS) of each gene was scanned for term-seq sites that were covered by a minimum of two reads in each of the three biological replicates. Because the average length of a terminator is ~20 to 25 nt (*56*), only 5′UTRs in which the distance between the TSS and the term-seq site was at least 70 nt were considered. Candidate regulators that displayed high term-seq density also across the gene body were discarded as likely degraded transcripts. In addition, candidates in which potential secondary TSSs could be detected downstream of the premature terminator were discarded. Because of specific regulator degradation/processing patterns, a handful of premature terminator sites were manually corrected to a nearby, less covered term-seq site if that site presented a stem-loop and polyU signature (corrections noted in table S2). To differentiate between known and previously unidentified regulators, all candidate elements were compared against the Rfam database (*33*) (Rfam 11.0 2012-07-19: AL009126.3, AL591824.1, and AE016830.1 for *B. subtilis*, *L. monocytogenes*, and *E. faecalis*, respectively) and the literature. All identified candidate regulators were independently compared with the online Rfam db.

Transcriptional read-through estimation by use of RNA-seq and term-seq

Term-seq average coverage across triplicates was calculated for the premature termination site and the full-length gene termination site with a span of 10 nt surrounding each terminator, and the fraction of full-length (gene) terminations out of all termination events was used as a measure of the transcriptional read-through (Fig. 3A). In cases in which the regulator controlled the transcription of a multi-gene operon, which contained internal TSSs in addition to the primary one, RNA-seq was used to determine read-through in the first gene (Fig. 4, C and F). RNA-seq coverage was used to measure the average read coverage over either the regulatory element or the gene, and the ratio between the two (gene-coverage divided by regulator-coverage) was used as an estimate for the short/long transcript ratio generated by regulator activity (Fig. 3A).

Term-seq analysis of in vitro transcribed RNA

Term-seq libraries were prepared as above by using *L. monocytogenes* RNA spiked in with 1 μl of 1:10 diluted ERCC RNA Spike-In Mix (Ambion, 4456740). Sequencing reads were mapped to the reference ERCC sequences, and the number of term-seq reads mapped to the exact spike-in RNA 3′ ends were counted and compared with the known RNA concentrations (fig. S2). Only spike-in RNAs with a known concentration of at least 1 attomoles (amol) and that were covered by at least one term-seq read ($n = 58$ RNAs) were used in the analysis.

Ribosome immunization ErmC 23S methylation

L. monocytogenes EGDe pAT18-cGFP (*53*) was grown overnight in BHI media and then diluted 1:200 into fresh BHI. ErmC expression was induced by incubating the cultures with 0.5 μg/ml erythromycin for 2 hours. The induced and the control (noninduced) samples were then exposed to 0.25 μg/ml of lincomycin or water as a control and incubated for 15 min. Bacteria were harvested by means of centrifugation, flash-frozen, and the

RNA was extracted, sequenced, and analyzed as described above.

Comparative sequence analysis of lmo0919 homologs

The Lmo0919 protein sequence was used to collect homologs in several Gram-positive bacteria (fig. S7). 5′UTRs were estimated as the 275 nt upstream top of the homologous gene and were analyzed by means of multiple sequence alignment and in silico RNA folding with Muscle (*57*) and with RNAfold (*54*), respectively. The upstream intergenic regions of *lmo0919* homologs identified in *Bacillus subtilis* subsp. *subtilis* str. 168, *Streptococcus gordonii* str. Challis substr. CH, *Enterococcus faecalis* V583, *Staphylococcus aureus* plasmid pVGA, and *Clostridium botulinum* CDC54075 were collected by using the Integrated Microbial Genomes database (IMG) (*58*) using, respectively, the following IMG gene IDs: 646317030, 640912864, 637415867, 643661871, and 2569227938.

Epifluorescence analysis

A colony of wild-type EGD-e and one of EGDe-rli53-GFP mutant *Listeria* were resuspended in 20 μL of phosphate-buffered saline and mounted on glass coverslips sealed with varnish. Samples were analyzed with an Axio Observer Z1 microscope (Zeiss) equipped with a spinning disk and an EvolveTM 512 EMCCD Camera (Photometrics). Images were acquired with a ×100 oil immersion objective and processed with MetaMorph (Universal Imaging) and Icy (Pasteur Institute).

Ribosome profiling (Ribo-seq)

L. monocytogenes EGDe and *L. innocua* Clip11262 were grown overnight in BHI media and then diluted 1:200 into fresh 200 ml BHI cultures. Cultures were grown to OD_{600} = 0.4 to 5 and then treated with either 0.5 μg/ml of lincomycin or water as a control for 15 min. The bacteria were collected via the rapid-filtration method (*43*) and flash-frozen in liquid nitrogen. Six hundred fifty microliters of lysis buffer containing 20 mM Tris 8.0, 10 mM MgCl2, 100 mM NH4Cl, 0.4% Triton X100, 0.1% NP-40, 1 mM chloramphenicol, and 100 U/ml DNase I (NEB, M0303) was dropped over liquid nitrogen and added to the pellets. Frozen cell pellets were pulverized in the MM301 Mixer mill (Retsch, Haan, Germany) by using a 10-ml stainless steel grinding jar and 12-mm grinding ball (Retsch) for five cycles, each at 30 Hz for 2 min, and chilled in liquid nitrogen between cycles. Frozen lysates were thawed on ice for 20 min and then centrifuged at 14,000 rpm for 10 min at 4°C, and the supernatant was collected. Micrococcal nuclease (MNase) digestion was performed by mixing 1 mg RNA with $CaCl_2$ (5 mM final), 6 μl Superase-In (Ambion), and 1.7 μl MNase (NEB, M0247). The reaction was incubated for 1 hour in 25°C with shaking and terminated by adding 5 mM EGTA (Sigma) and placing on ice. Monosomes were isolated by means of ultracentrifugation (Sw41 rotor, 35,000 rpm for 2.5 hours at 4°C) of the samples over 10 to 50% sucrose density gradient. Ribosomal footprints were collected as described in (*43*). Sequencing libraries were constructed by using NEBNext Small RNA Library Prep Set for Illumina (NEB, E7330) according to the manufacturer's instructions. The sequencing reads were adapter-trimmed by using the FASTX-Toolkit (fastx_clipper -Q33 -a AGATCGGAAGAGCACACGTCTGAACTCCAGTCAC -l 25 -c -n -v -i input_fastq_file), and inserts sized 25 to 40 nt were aligned to reference genome and analyzed as above.

For each ribosome profiling sample, we also sequenced the total RNA as following: 5 μg total RNA was fragmented as above for 5 min and then cleaned with SPRI as above and eluted in 16 μl of RNase-free H_2O. The fragmented RNA was end-repaired by using T4-polynucletide kinase (T4-PNK; NEB, M0201) by adding 2 μl T4-PNK 10X buffer and 2 μl T4-PNK and then incubating the reaction at 37°C for 2 hours. The enzyme was deactivated by incubating the sample at 75°C for 15 min, and the RNA was collected by means of isopropanol precipitation. The resulting RNA was rRNA-depleted as above, and libraries were prepared with the NEBNext Small RNA Library Prep Set for Illumina (NEB, E7330) kit as above.

Meta-term-seq

Oral plaque was collected from three healthy individuals by using a toothpick and then mixed into 1 ml of liquid BHI media, prewarmed to 37°C. The samples were vortexed for 10 s and then divided into tubes either containing BHI (control) or BHI supplemented with 1 μg/ml lincomycin and then incubated with shaking at 37°C for 15 min. Bacteria were pelleted via centrifugation and were then flash-frozen. RNA extraction and library construction were done as described above. Sequencing reads were mapped to all contigs larger than 2.5 kb taken from the 462 annotated genomes available at the Human Oral Microbiome Database (HOMD) (*46*). In cases in which multiple closely related strains of a single species were present in the database, only one representative genome was selected. Only bacterial genomes in which at least 10% of all protein-coding genes were covered by 10 or more uniquely mapped reads were selected for further analysis. Sequencing reads were remapped to the final database of 167 bacterial genomes. Term-seq and 5′ end sequencing reads were mapped by using the novoalign–r Random option. To identify lincomycin-responsive regulators, genes with a mapped TSS and premature term-seq site and that were covered by ≥50 RNA-seq reads and showed a >2.5-fold increase in expression in the lincomycin condition were selected for read-through calculation. Candidate regulators were classified as lincomycin-responsive if they increased their read-through by at least 2.5-fold after exposure to lincomycin and that had a read-through >10% in the lincomycin condition.

Construction of the phylogenetic tree in Fig. 6B was performed by using 16*S* rRNA sequences, taken from the Human Oral Microbiome Database (HOMD) or National Center for Biotechnology Information (NCBI), and by using the *phylogeny.fr* Web server with default parameters (*59*). The phylogenetic tree was deposited in the treebase online database (*treebase.org*) under accession no. 18921.

REFERENCES AND NOTES

1. W. Winkler, A. Nahvi, R. R. Breaker, Thiamine derivatives bind messenger RNAs directly to regulate bacterial gene expression. *Nature* **419**, 952–956 (2002). doi: 10.1038/nature01145; pmid: 12410317
2. M. Mandal, B. Boese, J. E. Barrick, W. C. Winkler, R. R. Breaker, Riboswitches control fundamental biochemical pathways in *Bacillus subtilis* and other bacteria. *Cell* **113**, 577–586 (2003). doi: 10.1016/S0092-8674(03)00391-X; pmid: 12787499
3. N. Sudarsan, J. K. Wickiser, S. Nakamura, M. S. Ebert, R. R. Breaker, An mRNA structure in bacteria that controls gene expression by binding lysine. *Genes Dev.* **17**, 2688–2697 (2003). doi: 10.1101/gad.1140003; pmid: 14597663
4. C. Yanofsky, Attenuation in the control of expression of bacterial operons. *Nature* **289**, 751–758 (1981). doi: 10.1038/289751a0; pmid: 7007895
5. T. J. Santangelo, I. Artsimovitch, Termination and antitermination: RNA polymerase runs a stop sign. *Nat. Rev. Microbiol.* **9**, 319–329 (2011). doi: 10.1038/nrmicro2560; pmid: 21478900
6. C. E. Dann 3rd *et al*., Structure and mechanism of a metal-sensing regulatory RNA. *Cell* **130**, 878–892 (2007). doi: 10.1016/j.cell.2007.06.051; pmid: 17803910
7. W. C. Winkler, S. Cohen-Chalamish, R. R. Breaker, An mRNA structure that controls gene expression by binding FMN. *Proc. Natl. Acad. Sci. U.S.A.* **99**, 15908–15913 (2002). doi: 10.1073/pnas.212628899; pmid: 12456892
8. W. C. Winkler, A. Nahvi, N. Sudarsan, J. E. Barrick, R. R. Breaker, An mRNA structure that controls gene expression by binding S-adenosylmethionine. *Nat. Struct. Biol.* **10**, 701–707 (2003). doi: 10.1038/nsb967; pmid: 12910260
9. N. Sudarsan *et al*., Riboswitches in eubacteria sense the second messenger cyclic di-GMP. *Science* **321**, 411–413 (2008). doi: 10.1126/science.1159519; pmid: 18635805
10. I. Irnov, W. C. Winkler, A regulatory RNA required for antitermination of biofilm and capsular polysaccharide operons in *Bacillales*. *Mol. Microbiol.* **76**, 559–575 (2010). doi: 10.1111/j.1365-2958.2010.07131.x; pmid: 20374491
11. E. Loh *et al*., A trans-acting riboswitch controls expression of the virulence regulator PrfA in *Listeria monocytogenes*. *Cell* **139**, 770–779 (2009). doi: 10.1016/j.cell.2009.08.046; pmid: 19914169
12. J. R. Mellin *et al*., Sequestration of a two-component response regulator by a riboswitch-regulated noncoding RNA. *Science* **345**, 940–943 (2014). doi: 10.1126/science.1255083; pmid: 25146292
13. J. S. Paige, T. Nguyen-Duc, W. Song, S. R. Jaffrey, Fluorescence imaging of cellular metabolites with RNA. *Science* **335**, 1194–1194 (2012). doi: 10.1126/science.1218298; pmid: 22403384
14. C. C. Fowler, E. D. Brown, Y. Li, Using a riboswitch sensor to examine coenzyme B(12) metabolism and transport in *E. coli*. *Chem. Biol.* **17**, 756–765 (2010). doi: 10.1016/j.chembiol.2010.05.025; pmid: 20659688
15. F. J. Isaacs, D. J. Dwyer, J. J. Collins, RNA synthetic biology. *Nat. Biotechnol.* **24**, 545–554 (2006). doi: 10.1038/nbt1208; pmid: 16680139
16. Y. Benenson, Synthetic biology with RNA: Progress report. *Curr. Opin. Chem. Biol.* **16**, 278–284 (2012). doi: 10.1016/j.cbpa.2012.05.192; pmid: 22676891
17. K. F. Blount, R. R. Breaker, Riboswitches as antibacterial drug targets. *Nat. Biotechnol.* **24**, 1558–1564 (2006). doi: 10.1038/nbt1268; pmid: 17160062
18. J. Mulhbacher *et al*., Novel riboswitch ligand analogs as selective inhibitors of guanine-related metabolic pathways. *PLOS Pathog.* **6**, e1000865 (2010). pmid: 20421948
19. R. R. Breaker, Prospects for riboswitch discovery and analysis. *Mol. Cell* **43**, 867–879 (2011). doi: 10.1016/j.molcel.2011.08.024; pmid: 21925376
20. Z. Weinberg *et al*., Comparative genomics reveals 104 candidate structured RNAs from bacteria, archaea, and their metagenomes. *Genome Biol.* **11**, R31 (2010). doi: 10.1186/gb-2010-11-3-r31; pmid: 20230605
21. R. Sorek, P. Cossart, Prokaryotic transcriptomics: A new view on regulation, physiology and pathogenicity. *Nat. Rev. Genet.* **11**, 9–16 (2010). doi: 10.1038/nrg2695; pmid: 19935729

22. M. Güell, E. Yus, M. Lluch-Senar, L. Serrano, Bacterial transcriptomics: What is beyond the RNA horiz-ome? *Nat. Rev. Microbiol.* **9**, 658–669 (2011). doi: 10.1038/nrmicro2620; pmid: 21836626
23. Materials and methods are available as supplementary materials on *Science* Online.
24. O. Wurtzel *et al*., A single-base resolution map of an archaeal transcriptome. *Genome Res.* **20**, 133–141 (2010). doi: 10.1101/gr.100396.109; pmid: 19884261
25. O. Wurtzel *et al*., Comparative transcriptomics of pathogenic and non-pathogenic Listeria species. *Mol. Syst. Biol.* **8**, 583 (2012). doi: 10.1038/msb.2012.11; pmid: 22617957
26. J. P. Sarsero, E. Merino, C. Yanofsky, A Bacillus subtilis operon containing genes of unknown function senses tRNATrp charging and regulates expression of the genes of tryptophan biosynthesis. *Proc. Natl. Acad. Sci. U.S.A.* **97**, 2656–2661 (2000). doi: 10.1073/pnas.050578997; pmid: 10706627
27. C. Holmberg, L. Rutberg, An inverted repeat preceding the *Bacillus subtilis glpD* gene is a conditional terminator of transcription. *Mol. Microbiol.* **6**, 2931–2938 (1992). doi: 10.1111/j.1365-2958.1992.tb01752.x; pmid: 1479885
28. R. J. Turner, Y. Lu, R. L. Switzer, Regulation of the *Bacillus subtilis* pyrimidine biosynthetic (pyr) gene cluster by an autogenous transcriptional attenuation mechanism. *J. Bacteriol.* **176**, 3708–3722 (1994).pmid: 8206849
29. Y. Fujita, Carbon catabolite control of the metabolic network in *Bacillus subtilis*. *Biosci. Biotechnol. Biochem.* **73**, 245–259 (2009). doi: 10.1271/bbb.80479; pmid: 19202299
30. E. Reilman, R. A. Mars, J. M. van Dijl, E. L. Denham, The multidrug ABC transporter BmrC/BmrD of *Bacillus subtilis* is regulated via a ribosome-mediated transcriptional attenuation mechanism. *Nucleic Acids Res.* **42**, 11393–11407 (2014). doi: 10.1093/nar/gku832; pmid: 25217586
31. M. Naville, D. Gautheret, Premature terminator analysis sheds light on a hidden world of bacterial transcriptional attenuation. *Genome Biol.* **11**, R97 (2010). doi: 10.1186/gb-2010-11-9-r97; pmid: 20920266
32. R. Ohki, K. Tateno, T. Takizawa, T. Aiso, M. Murata, Transcriptional termination control of a novel ABC transporter gene involved in antibiotic resistance in *Bacillus subtilis*. *J. Bacteriol.* **187**, 5946–5954 (2005). doi: 10.1128/JB.187.17.5946-5954.2005; pmid: 16109936
33. E. P. Nawrocki *et al*., Rfam 12.0: Updates to the RNA families database. *Nucleic Acids Res.* **43** (D1), D130–D137 (2015). doi: 10.1093/nar/gku1063; pmid: 25392425
34. C. Maertens de Noordhout *et al*., The global burden of listeriosis: A systematic review and meta-analysis. *Lancet Infect. Dis.* **14**, 1073–1082 (2014). doi: 10.1016/S1473-3099(14)70870-9; pmid: 25241232
35. I. G. Sava, E. Heikens, J. Huebner, Pathogenesis and immunity in enterococcal infections. *Clin. Microbiol. Infect.* **16**, 533–540 (2010). doi: 10.1111/j.1469-0691.2010.03213.x; pmid: 20569264
36. A. Toledo-Arana *et al*., The Listeria transcriptional landscape from saprophytism to virulence. *Nature* **459**, 950–956 (2009). doi: 10.1038/nature08080; pmid: 19448609
37. M. A. Mraheil *et al*., The intracellular sRNA transcriptome of *Listeria monocytogenes* during growth in macrophages. *Nucleic Acids Res.* **39**, 4235–4248 (2011). doi: 10.1093/nar/gkr033; pmid: 21278422
38. T. P. Burke *et al*., *Listeria monocytogenes* is resistant to lysozyme through the regulation, not the acquisition, of cell wall-modifying enzymes. *J. Bacteriol.* **196**, 3756–3767 (2014). doi: 10.1128/JB.02053-14; pmid: 25157076
39. J. H. Kwak, E. C. Choi, B. Weisblum, Transcriptional attenuation control of ermK, a macrolide-lincosamide-streptogramin B resistance determinant from Bacillus licheniformis. *J. Bacteriol.* **173**, 4725–4735 (1991). pmid: 1713206
40. A. Aakra *et al*., Transcriptional response of *Enterococcus faecalis* V583 to erythromycin. *Antimicrob. Agents Chemother.* **49**, 2246–2259 (2005). doi: 10.1128/AAC.49.6.2246-2259.2005; pmid: 15917518
41. O. Chesneau, H. Ligeret, N. Hosan-Aghaie, A. Morvan, E. Dassa, Molecular analysis of resistance to streptogramin A compounds conferred by the Vga proteins of staphylococci. *Antimicrob. Agents Chemother.* **49**, 973–980 (2005). doi: 10.1128/AAC.49.3.973-980.2005; pmid: 15728891
42. D. N. Wilson, The A-Z of bacterial translation inhibitors. *Crit. Rev. Biochem. Mol. Biol.* **44**, 393–433 (2009). doi: 10.3109/10409230903307311; pmid: 19929179
43. G. W. Li, E. Oh, J. S. Weissman, The anti-Shine-Dalgarno sequence drives translational pausing and codon choice in bacteria. *Nature* **484**, 538–541 (2012). doi: 10.1038/nature10965; pmid: 22456704
44. T. Tenson, M. Lovmar, M. Ehrenberg, The mechanism of action of macrolides, lincosamides and streptogramin B reveals the nascent peptide exit path in the ribosome. *J. Mol. Biol.* **330**, 1005–1014 (2003). doi: 10.1016/S0022-2836(03)00662-4; pmid: 12860123
45. F. E. Dewhirst *et al*., The human oral microbiome. *J. Bacteriol.* **192**, 5002–5017 (2010). doi: 10.1128/JB.00542-10; pmid: 20656903
46. T. Chen *et al*., The Human Oral Microbiome Database: A web accessible resource for investigating oral microbe taxonomic and genomic information. *Database (Oxford)* **2010**, baq013 (2010). doi: 10.1093/database/baq013; pmid: 20624719
47. C. Méndez, J. A. Salas, The role of ABC transporters in antibiotic-producing organisms: Drug secretion and resistance mechanisms. *Res. Microbiol.* **152**, 341–350 (2001). doi: 10.1016/S0923-2508(01)01205-0; pmid: 11421281
48. Q. Zhao *et al*., Influence of the TonB energy-coupling protein on efflux-mediated multidrug resistance in Pseudomonas aeruginosa. *Antimicrob. Agents Chemother.* **42**, 2225–2231 (1998). pmid: 9736539
49. J. Davies, G. D. Wright, Bacterial resistance to aminoglycoside antibiotics. *Trends Microbiol.* **5**, 234–240 (1997). doi: 10.1016/S0966-842X(97)01033-0; pmid: 9211644
50. A. L. Starosta, J. Lassak, K. Jung, D. N. Wilson, The bacterial translation stress response. *FEMS Microbiol. Rev.* **38**, 1172–1201 (2014). doi: 10.1111/1574-6976.12083; pmid: 25135187
51. S. Douthwaite, P. F. Crain, M. Liu, J. Poehlsgaard, The tylosin-resistance methyltransferase RlmA(II) (TlrB) modifies the N-1 position of 23S rRNA nucleotide G748. *J. Mol. Biol.* **337**, 1073–1077 (2004). doi: 10.1016/j.jmb.2004.02.030; pmid: 15046978
52. M. Arnaud, A. Chastanet, M. Débarbouillé, New vector for efficient allelic replacement in naturally nontransformable, low-GC-content, Gram-positive bacteria. *Appl. Environ. Microbiol.* **70**, 6887–6891 (2004) pMAD. doi: 10.1128/AEM.70.11.6887-6891.2004; pmid: 15528558
53. D. Balestrino *et al*., Single-cell techniques using chromosomally tagged fluorescent bacteria to study *Listeria monocytogenes* infection processes. *Appl. Environ. Microbiol.* **76**, 3625–3636 (2010). doi: 10.1128/AEM.02612-09; pmid: 20363781
54. R. Lorenz *et al*., ViennaRNA Package 2.0. *Algorithms Mol. Biol.* **6**, 26 (2011). doi: 10.1186/1748-7188-6-26; pmid: 22115189
55. G. E. Crooks, G. Hon, J.-M. Chandonia, S. E. Brenner, WebLogo: A sequence logo generator. *Genome Res.* **14**, 1188–1190 (2004). doi: 10.1101/gr.849004; pmid: 15173120
56. M. J. L. de Hoon, Y. Makita, K. Nakai, S. Miyano, Prediction of transcriptional terminators in Bacillus subtilis and related species. *PLOS Comput. Biol.* **1**, e25 (2005). doi: 10.1371/journal.pcbi.0010025; pmid: 16110342
57. R. C. C. Edgar, MUSCLE: Multiple sequence alignment with high accuracy and high throughput. *Nucleic Acids Res.* **32**, 1792–1797 (2004). doi: 10.1093/nar/gkh340; pmid: 15034147
58. V. M. Markowitz *et al*., IMG: The Integrated Microbial Genomes database and comparative analysis system. *Nucleic Acids Res.* **40**, D115–D122 (2012). pmid: 22194640
59. A. Dereeper *et al*., Phylogeny.fr: Robust phylogenetic analysis for the non-specialist. *Nucleic Acids Res.* **36** (Web Server), W465–W469 (2008). doi: 10.1093/nar/gkn180; pmid: 18424797

ACKNOWLEDGMENTS

We thank O. Wurtzel, I. Karunker, S. Doron, G. Amitai, G. Ofir, A. Millman, Y. Voichek, S. Melamed, and R. Nir-Paz for insightful discussion. R.S. was supported, in part, by the Israel Science Foundation (personal grant 1303/12 and I-CORE grant 1796/12), the European Research Council (ERC)–Starting Grants program (grant 260432), Human Frontier Science Program (grant RGP0011/2013 to R.S. and P.C), the Abisch-Frenkel foundation, the Pasteur-Weizmann council grant (to R.S and P.C), the Minerva Foundation, the Leona M. and Harry B. Helmsley Charitable Trust, and by a Deutsch-Israelische Projektkooperation grant from the Deutsche Forschungsgemeinschaft. P.C was supported by an ERC–Advanced Grants grant (BacCellEpi, #670823). Reference IRB for the microbiome analysis is 0315-15-HMO. Sequencing data was deposited in the European Nucleotide Database (ENA), accession no. PRJEB12568. D.D. and R.S. are inventors on U.S. provisional patent application 62/200,662.

SUPPLEMENTARY MATERIALS

www.sciencemag.org/content/352/6282/aad9822/suppl/DC1
Materials and Methods
Figs. S1 to S11
Tables S1 to S11

2 December 2015; accepted 24 February 2016
10.1126/science.aad9822